# Design-for-Testing for Improved Remanufacturability

**Katherine M. M. Tant[1§], Anthony J. Mulholland[1], Andrew Curtis[2], Winifred L. Ijomah[3]**

[1]Department of Mathematics and Statistics, University of Strathclyde, Livingstone Tower, Richmond Street, Glasgow, UK
[2]School of Geosciences, University of Edinburgh, Grant Institute, Kings Buildings, Edinburgh, UK
[3]Department of Design, Manufacture and Engineering Management, University of Strathclyde, James Weir Building, Montrose Street, Glasgow, U.K.

[§]Corresponding author

Email addresses:
KMMT: katy.tant@strath.ac.uk
AJM: anthony.mulholland@strath.ac.uk
AC: andrew.curtis@ed.ac.uk
WLI: w.l.ijomah@strath.ac.uk

## Abstract

By definition, a remanufactured product must perform to the same (or higher) level as the original product, and must therefore be issued a warranty of the same (or longer) duration. However, many components of remanufactured products will have been subjected to regular stresses in their first cycle of use and may exhibit unseen signs of damage at a microstructural level. This may not affect the remanufactured product's performance initially but could cause it to fail before its renewed warranty expires. To combat this, we propose that the integrity of individual components is assessed non-destructively before storage. However, lack of remanufacture specific tools and techniques; particularly non-destructive tools, are major hindrances. Furthermore, ease of non-destructive testing (NDT) is not currently a consideration in the design of components; components with complex geometries may therefore be difficult to test. This paper presents, for the first time, a framework for including NDT suitability as a design criterion at the outset in the component's lifecycle, where the geometry and surface accessibility of the component are optimised for future assessment. Ensuring that components can be easily inspected would not only allow increased confidence in the structural integrity of remanufactured products, but it would also extend the range of products suitable for remanufacturing. This paper serves as a proof of concept, examining simple inspection scenarios in order to demonstrate how the shape of components and data acquisition geometries can adversely affect the coverage of ultrasonic NDT.

## Introduction

The majority of remanufacturing processes described in the literature follow a similar procedure: the cores are stripped; components are cleaned, visually assessed, remanufactured and stored; then the product is rebuilt and its performance tested [1,2,3]. Due to a shortage of remanufacture-specific tools and expertise for the non-destructive inspection of these components [4], their integrity is often assessed by their exterior

appearance and functional performance. Although it might meet initial performance criteria, interior damage of the structure caused by the strains and stresses experienced in the component's first life-cycle could lead to a shorter lifetime than predicted [5]. Full microstructural assessment at the remanufacturing stage would allow increased confidence in the component's integrity and would allow remanufacturing processes to be more readily rolled out to components in high stress environments such as those found in the aerospace and energy industries.

Non-destructive testing (NDT) is an umbrella term for a wide range of analysis techniques used to evaluate and characterise components non-invasively [6]. They are employed to detect defects, take thickness measurements and characterise the internal material properties of components. Ultrasonic NDT uses high frequency mechanical waves to inspect components, ensuring that they operate reliably without compromising their integrity [7]. It has grown in popularity within the NDT industry in recent years due to the relatively inexpensive and portable equipment it requires, and its potential for automation and real-time results [8]. There already exists a large and varied literature on the applications of ultrasonic NDT, and the imaging algorithms required to process the collected ultrasonic data are under constant development [9,10]. However, complex component geometries and composite material microstructures still present significant challenges for the successful application of ultrasonic NDT.

To combat this difficulty and improve the ease with which NDT can be applied within the remanufacturing process, we propose a framework for including NDT suitability as a consideration in the component's initial design. By varying the shape and distribution of material within a component, we can maximise the coverage of the ultrasonic field over the structure and minimise the area of 'dead zones' (areas which are not probed by the transmitted wave), thus improving our ability to reliably image internal features of the component.

Optimal structural design is of particular importance to the aerospace, automotive and civil engineering industries [11]. It is typically used to produce economical, lightweight and robust design solutions whilst adhering to size, weight and topological constraints. Often, an optimisation problem requires the minimisation of more than one variable. For example, companies may often want to look for a structural solution which is both lightweight and low-cost. Thus we have to deal with a multi-objective design optimisation [12]. These objectives can typically be prioritised, resulting in a multi-level optimisation problem in which a set of solutions for the high priority objectives are sought before these are then optimised with regard to the lower priority objectives. In this paper we propose that NDT suitability is introduced as a secondary objective where the subset of solutions shown to be optimal for the existing objectives within a design process are subjected to an optimisation scheme which focusses on maximising the coverage of the ultrasonic field throughout the component given the restrictions on access to its surface. A multi-level optimisation framework, in which both the shape of the component and the location of the sensors are optimised, is presented. Inspection scenarios are simulated for a range of irregularly shaped components as a proof of concept, demonstrating how the extent of the array aperture and the convexity and surface smoothness of the component can affect the acoustic pressure coverage. To the authors' knowledge, this is the first time that the ease of with which a component can be non-destructively evaluated has been suggested as a consideration in the design process and as such, novel cost functions for the optimisation framework, based on quantification of the coverage of the pressure field, have been developed. It is hoped that by implementing this approach, not only will the success of in service inspections be enhanced, but the range of

products which are suitable for remanufacturing at the end of their first life cycle will be extended.

# Methods

### Optimisation of the Component Design

When a component with domain $\Omega$ is submitted to ultrasonic NDT, a mechanical force is typically induced at points $x$ on the component's boundary, $\partial\Omega$. The coverage of the resulting acoustic pressure field throughout the component is dependent on the shape and material properties of the component. The pressure felt at a point $y \in \Omega$, denoted here as $z(y,t)$, can be written

$$z(y,t) = F(y,t,\theta,s,x) \tag{1}$$

where $F$ is some model of the wave process which is dependent on time $t$, material properties $\theta$, some parameterisation $s$ of $\partial\Omega$ and the positioning of the sensor (or sensors) $x$. In this work, a finite element simulation of the wave propagation will be used as our model $F$ [13]. To obtain a map, $M(y)$, of the coverage, the maximum pressure observed over all $t$ at each point $y$ is plotted. The coverage map is used as a proxy to measure the ease of NDT, and is quantified here by

$$\phi = \min_{y\in\Omega} M(y) = \min_{y\in\Omega} \max_{t\in R^+} z(y,t). \tag{2}$$

Note, alternative measures of the map $M$ may be explored; for example the mean value of the pressure field throughout the component, or the number of points in the domain $\Omega$ which lie above some pre-determined threshold, relative to the total number of points, are examined in the work below.

By introducing more sources at different locations on the component's boundary, we can modify the overall coverage of the component as we are effectively illuminating it from an increased range of angles. To incorporate this, we introduce a probability density function $\xi(x)$ which describes the likelihood that a sensor is placed at point $x$ on the component boundary (see Figure 1). Taking, for the moment, the material properties $\theta$ to be fixed, we now have all of the components required to define the design criterion function:

$$\Psi(\xi(x),s) = \min_{y\in\Omega} \max_{t\in R^+} \int_{\partial\Omega} z(y,t;\theta,s,x)\xi(x)d\ .x \tag{3}$$

Here, integrating over $x$ allows us to effectively sum the contributions by all sources, and this is weighted by the probability density function $\xi(x)$ to give an expected value. As before, the maximum value at $y$ over all $t$ is taken (this is effectively map $M$) of which the minimum is taken as the coverage measure $\Psi(\xi(x),s)$. As we are optimising over two parameters: the shape of the component and the placement of sensors, we adopt a multi-level optimisation approach. To clarify this approach, we initially isolate the secondary optimisation.

**Problem 1: Calculating optimal sensor placement (the lower level optimisation)**

For a given component for which the material properties $\theta$ and shape $s$ are known, we wish to find the optimal sensor placement $\xi^*(x)$

$$\xi^*(x) = \arg\max_{\xi \in \Phi(\partial\Omega(s))} \Psi(\xi(x); s), \tag{4}$$

where $\Phi(\partial\Omega(s))$ is the set of admissible source locations for the given shape parameterisation $s$. Using a Markov chain Monte Carlo (MCMC) method coupled with Metropolis-Hastings criterion [14], we can iterate over the model space, changing the distribution of sensors $\xi(x)$ over the component's surface to maximise $\Psi(\xi(x); s)$.

The optimisation discussed in Problem 1, is applied when the shape parameterisation $s$ is known, and so, we apply this once we have obtained an optimal component geometry. This brings us to the multi-level optimisation scheme.

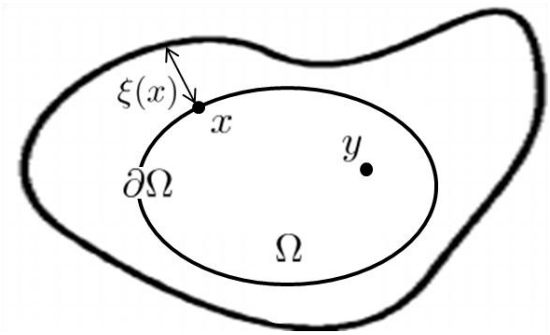


**Figure 1:** Schematic of an arbitrary component geometry **Ω**. The outer line depicts the probability that a source will be positioned at that point on the boundary – i.e. in this case it is more likely that a source is positioned at the top right of the domain than the bottom left of the domain.

**Problem 2: Optimising component design and sensor placement**

We assume that the material properties $\theta$ are known throughout the domain Ω. We wish to maximise $\Psi(\xi(x), s)$ by finding the optimal admissible boundary design $\partial\Omega(s^*)$ and the optimal source placement $\xi^*(x)$ using a multi-level optimisation scheme. Firstly, we find

$$\partial\Omega(s^*) = \arg\max_{\partial\Omega(s) \in D} \Psi(\xi(x), s), \tag{5}$$

where $D$ is the set of admissible component geometry boundaries (subject to the initial design constraints set by the product manufacturer). To find $\partial\Omega(s^*)$, we use an MCMC algorithm where the function $s$ is perturbed to modify the component's shape. For each putative component geometry, the optimal placement of sensors on its boundary is computed as in equation (4). Thus we obtain a component geometry which lies within the initial design constraints and, when inspected by sensors placed according to $\xi^*(x)$, maximises our ability to successfully test the component non-destructively.

### Simulation of the Ultrasonic Inspection of a given Component Design

Having set up this design optimisation framework for ultrasonic array NDT, we now demonstrate the effects that the sensor placement $\xi(x)$ and component boundary $\partial\Omega(s)$ have on the coverage $\Psi$. The software package PZFlex [13] was identified as the ideal environment to examine the effects of inspection aperture and component design on the

coverage of the induced ultrasonic field. Using this finite element software, we were able to simulate the ultrasonic inspection of irregularly shaped components. Although we initially work within a two dimensional framework, PZFlex has the capability to read in CAD files of 3D components [15] and so the framework developed now can easily be extended to more complex design scenarios in the future.

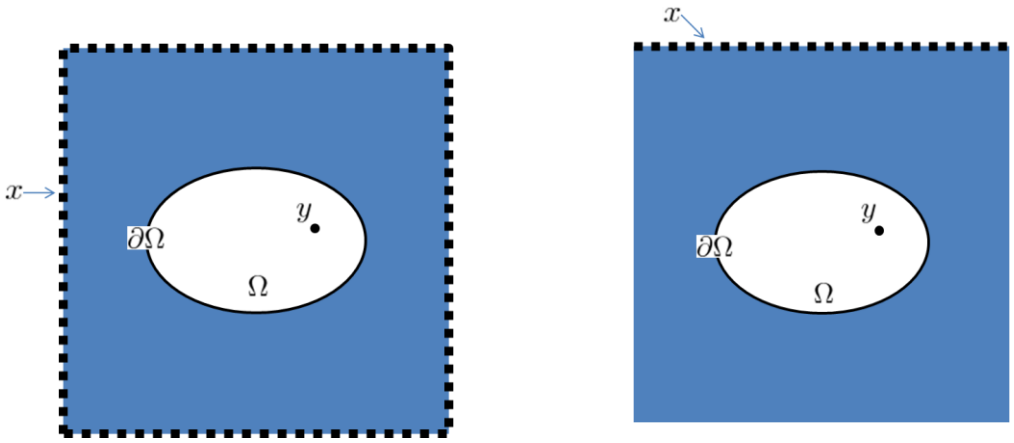


(a) (b)

**Figure 2**: Two different inspection scenarios where the dotted line represents the distribution of ultrasonic array sources: (a) is referred to a full aperture inspection and (b) is referred to as a limited aperture or single sided inspection.

Two different inspection scenarios were modelled. The first was a four sided inspection, where an array of point sources were placed on each side of the two-dimensional square domain, encircling the component under inspection and providing a full aperture interrogation (see Figure 2 (a)). The second scenario modelled a linear array of point sources placed on a single side of the inspection domain (Figure 2 (b)). This single-sided inspection better represents the scenarios faced by NDT operators in industry where only a sub-region of the surface can be accessed. In both cases, the elements were fired simultaneously to induce plane waves and inject the maximum amount of energy into the system. Note that here the sensors are not placed on the component boundary but are instead placed in the water surrounding the component. This is known as immersion testing and allows for testing of irregularly shaped components by standard phased array equipment. The method presented above could easily be extended to consider this case by relaxing the constraint that states $x$ lies on the boundary of the component.

# Results

### Effects of Component Design on Ultrasonic Coverage

To begin, we examine the simplest case and compare the ultrasonic coverage of a steel disc placed in water against that of a rectangular steel block placed in water (the geometries are shown in Figure 3 (a) and (d)). Initially, a one sided inspection was simulated where a plane wave was induced at the top of the domain. The wave travels through the water host until it reaches the component where some energy penetrates its surface and, due to the mismatch in impedance between the water and steel, a high proportion of the energy is reflected or redirected around the component. The results are shown in Figures 3 (b) and (e) for the rectangular block and disc respectively, and both are plotted over a dynamic range of 30dB. The maps are quantified by the mean, variance,

minimum amplitude and percentage of pixels which lie above the -20dB threshold (see Table 1) and it can be concluded that the coverage is better in the rectangular sample. The results arising from a full aperture inspection are shown in images (c) and (f) and again, from the values in Table 1, the rectangular component exhibits a higher pressure field throughout. Note in this case however, that if we take the variance of the pressure field as a measure of the uniformity of the coverage, we observe that the disc exhibits a more even coverage than the rectangular block. However, the mean value tells us that the coverage is of lower quality in the disc case. This can be attributed to the fact that its rounded boundaries guide the pressure wave around the object, thus reducing penetration and lessening the component's coverage.

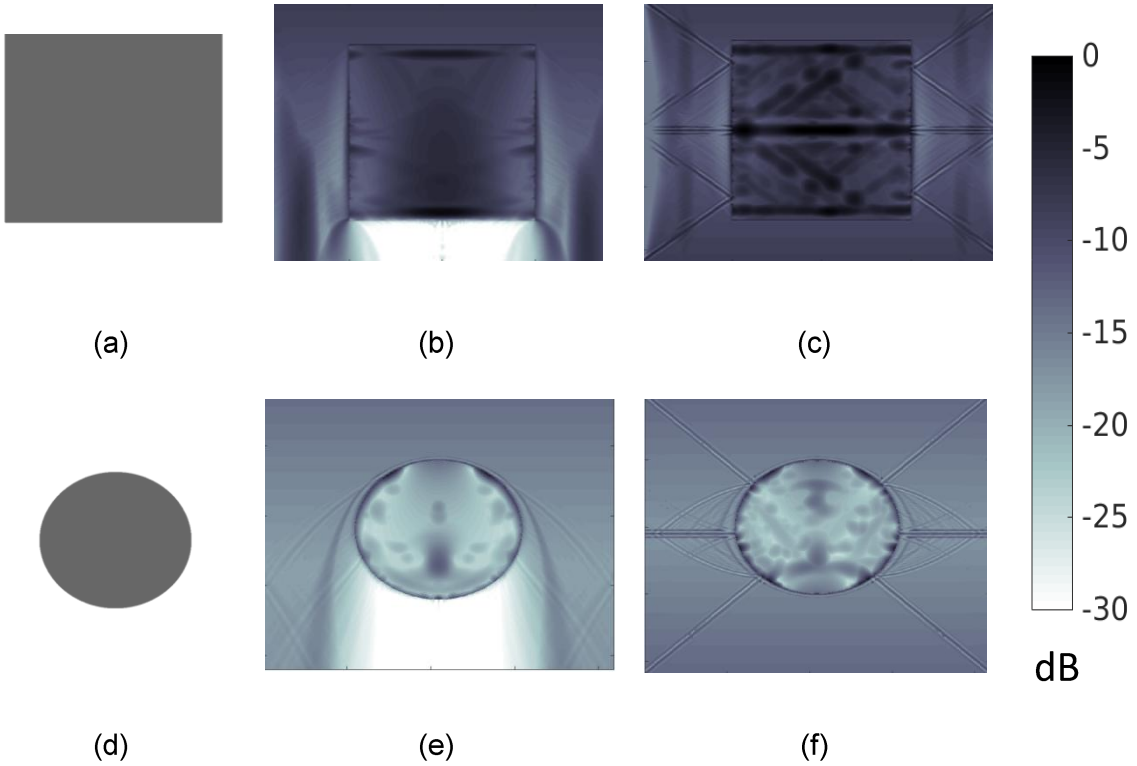


**Figure 3**: The ultrasonic coverage of simple components was examined. Image (a) shows a rectangular steel block and images (b) and (c) show the maximum acoustic pressure measured at each point in the domain for the limited and full apertures respectively. Image (d) shows a steel disc and images (e) and (f) show the maximum acoustic pressure measured at each point in the domain for the limited and full apertures respectively.

**Table 1** Quantitative measures of the coverage maps plotted in Figure 3.

| Geometry | Inspection Aperture | Mean (dB) | Var (dB) | Min (dB) | >-20db (%) |
|---|---|---|---|---|---|
| (a) | Limited | -7.6 | 8 | -17.8 | 100 |
| | Full | -7 | 11.5 | -13 | 100 |
| (d) | Limited | -19 | 9 | -23.5 | 48 |
| | Full | -17 | 9.3 | -24 | 64 |

The next step in understanding important aspects of component and experimental design was to study more complex component geometries. Three examples are shown in

Figures 4 (a), (b) and (c) where more irregularly shaped components are studied. The component shown in Figure 4 (a) was firstly inspected by a single plane wave induced at the top of the domain. As most of the upper surface lies perpendicular to the wave front direction, a large proportion of the energy penetrates the surface of the component. The energy appears to concentrate in the central, narrow area of the component and high amplitudes can be observed at its inner corners. From initial observations, these inverted corners seem to trap the energy within the component by diffracting outgoing energy and redirecting it internally. The same phenomenon is observed in the full aperture case (Figure 4 (g)). When the corners are rounded out, as in geometry 4 (b), this effect is lessened. Instead, the amplitudes are highest at the rounded surface of the component as observed previously in the disc case, and the coverage within the component deteriorates (Figures 4 (e) and (h)). Quantitative measures of the coverage are recorded in Table 2 and the values for the limited aperture and full aperture cases can be compared. Note that there is an improvement in coverage in each case when the full aperture is employed however this must be tempered by the fact that four times as much energy is entering the system.

Another way the ultrasonic coverage was altered resulted from placing the sensors at the left hand side of the domain. Much of the energy is trapped in the left vertical bar of the component as the wave is reflected off the inner steel-water interface. The same result is observed in the case shown in Figure 4 (k), but to a lesser extent due to the curved surface (less energy is transmitted into the component to start with). In both cases, the vertical bar on right hand side receives very little coverage and would be considered a 'dead zone'.

Finally, a crescent shaped component was examined (Figure 4 (c)). As observed in all previous examples, the curved surface leads to poor coverage of the component. Naturally, when the concave curved surface is illuminated by the plane wave (as in the full aperture case shown in Figure 4 (i)) a focal point of energy outside of the component is created, which is detrimental to our purpose.

**Table 2** Comparing the coverage afforded by three different inspections for geometries (a), (b) and (c) in Figure 4.

| | Sources at top of the domain | | | Full Aperture | | | Sources at left of domain | | |
|---|---|---|---|---|---|---|---|---|---|
| | (a) | (b) | (c) | (a) | (b) | (c) | (a) | (b) | (c) |
| Mean (dB) | -17.3 | -23 | -23.7 | -14.7 | -20 | -19.4 | -23.5 | -27.9 | -33.8 |
| Var (dB) | 18 | 18.7 | 36.3 | 10.4 | 10.16 | 15.5 | 21.6 | 25.2 | 19.5 |
| Min (dB) | -46 | -60 | -54.4 | -26.2 | -57 | -41.1 | -40.5 | -62 | -58 |
| >-20dB (%) | 85 | 21 | 20.4 | 99.3 | 38.2 | 54 | 7.8 | 0.3 | 0.2 |

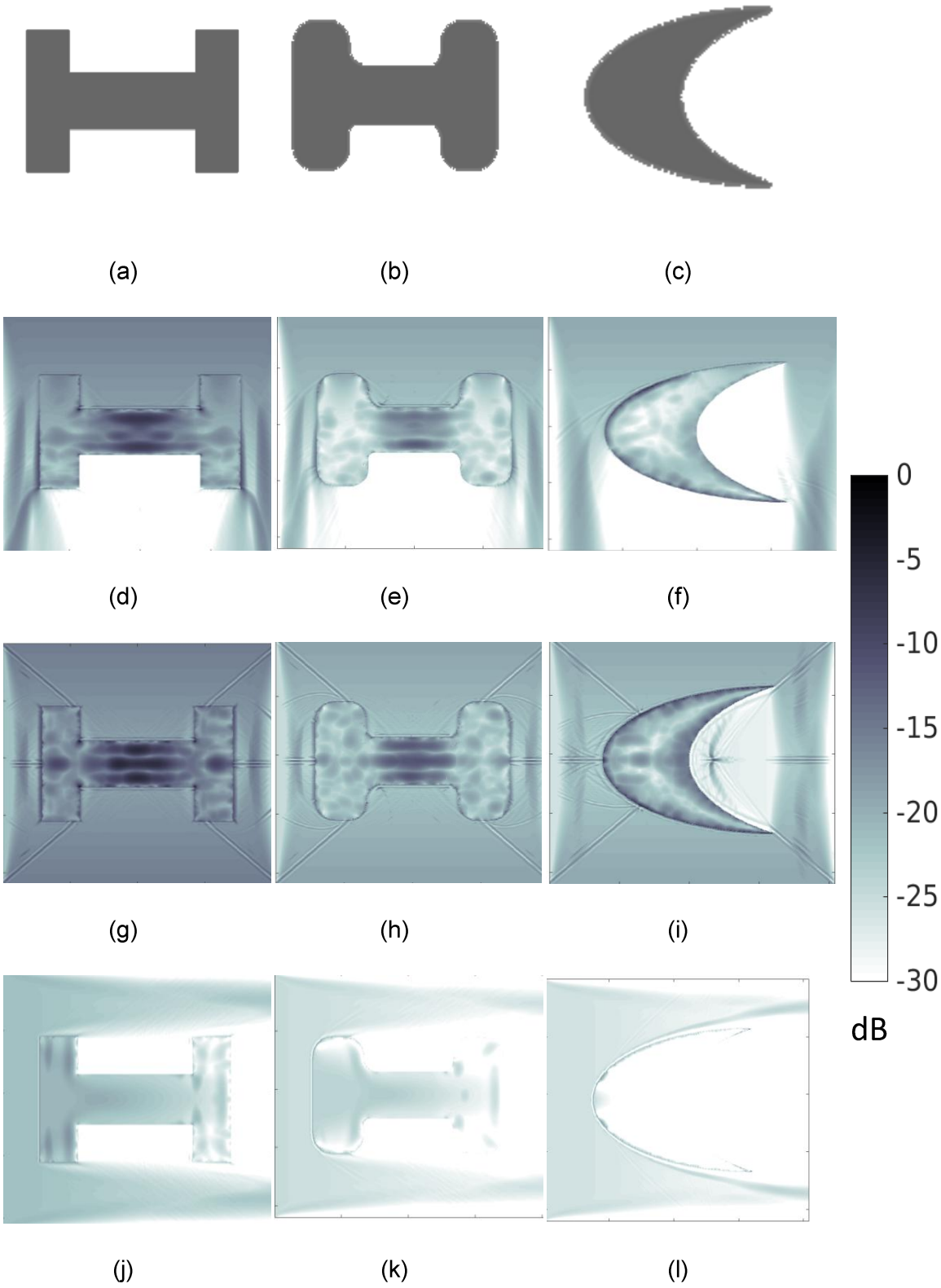


**Figure 4**: Images (a-c) show the irregularly shaped components input into the finite element (PZFlex) inspection simulation. Images (d-f) plot the maximum acoustic pressure at each point in the domain for a single-sided inspection where the incident plane wave is released at the top of the domain, (g-i) for the full aperture inspection and (j-l) for the single sided inspection where the incident wave travels from left to right..

## Conclusions

The primary aim of this paper was to present a mathematical framework for including ease of NDT as a design consideration, and to demonstrate that by altering a component's shape and data acquisition geometry, the coverage of the pressure field can be adjusted. It is hoped that by considering NDT suitability in the design process, not only will the success of in service inspections be enhanced, but the range of products suitable for remanufacturing will be extended.

A multi-level optimisation scheme which maximises the coverage of the ultrasonic field by perturbing the component's shape and subsequently assessing the optimal placement of sensors on the component's boundary is proposed. To better understand how these factors affect the coverage of the ultrasonic field, simulations of limited and full aperture inspection scenarios were run in the software package PZFlex. The coverage was quantified using the mean value of the coverage map, the variance, the minimum amplitude of the field and the percentage of points in the domain which lie above a threshold (chosen here as -20dB). Five different component geometries were examined in this way and it was shown that the presence of curved boundaries prohibited the penetration of the wave energy at the surface of the component (the external pressure field flowed around the boundary), whilst surfaces parallel to the incident wave field resulted in higher amplitude coverage throughout the component. Additionally, coverage was improved when a full aperture was employed (as expected) but also varied dramatically depending on which surface lay parallel to the incident plane wave. Having proposed this framework and defined some measures for quantifying the coverage, the next step will be to implement the optimisation strategy on simple, yet industrially relevant, component geometries. The method will then be extended to include a third nested optimisation in which the distribution of the material properties $\theta$ will be considered.

## Authors' contributions

Each author contributed to the development of the novel concept central to this paper. The simulations were run by KMMT.

## Acknowledgements

This work was funded by the Engineering and Physical Sciences Research Council (grant number EP/P005268/1). The authors would like to thank the team at PZFlex (Glasgow office) for their continued support.

## References

1. Lund RT: Remanufacturing: The experience of the U.S.A. and implications for the Developing Countries. *World Bank Technical Paper No. 3*,1984.
2. Ridley SJ: Increasing the Efficiency of Engine Remanufacture by Optimising Pre-Processing Inspection – A comprehensive study of 2196 engines at Caterpillar Remanufacturing in the UK. *PhD Dissertation: The University of Strathclyde*, UK, 2013.
3. Ijomah WL, McMahon CA, Hammond GP, Newman ST: Development of design for remanufacturing guidelines to support sustainable manufacturing. *Robotics and Computer-Integrated Manufacturing* 2007, 712-719.

4. Hammond R, Amezquita T, Bras B: Issues in the automotive parts remanufacturing industry: a discussion of results from surveys performed among remanufacturers. *Engineering Design and Automation* 4 1998, 27-46.
5. Koul AK, Castillo R: Assessment of service induced microstructural damage and its rejuvenation in turbine blades. *Metallurgical Transactions A* 1988, 2049-2066.
6. Raj B, Jayakumar T, Thavasimuthu M. *Practical non-destructive testing.* Woodhead Publishing, 2002.
7. Schmerr, LW. *Fundamentals of ultrasonic nondestructive evaluation.* Springer, 2016.
8. Brown RH, Pierce SG, Collison, I et al: Automated full matrix capture for industrial processes. *41st Annual Review of Progress in Quantitative Nondestructive Evaluation: Volume 34,* 2015, vol. 1650, 1967-1976.
9. Fan C, Caleap M, Pan M, Drinkwater BW: A comparison between ultrasonic array beamforming and super resolution imaging algorithms for non-destructive evaluation. *Ultrasonics,* 2014, 54(7):1842-50.
10. Tant KMM, Galetti E, Mulholland AJ, Curtis A, Gachagan A: Mapping the material microstructure of safety critical components using ultrasonic phased arrays. in *IEEE International Ultrasonics Symposium (IUS),* 2016, France, 18-21 September.
11. Farkas J, Jármai K. Analysis and optimum design of metal structures. *CRC Press.* 1997.
12. Farkas J, Jármai K:. *Design and optimization of metal structures.* 2008, Elsevier.
13. PZFlex. Thornton Tomasetti Defence Ltd 6th Floor South, 39 St Vincent Place, Glasgow, Scotland, G1 2ER, United Kingdom; 2017.
14. Aster RC, B. Borchers B, Thurber CH, *Parameter Estimation and Inverse Problems*, 2005, Elsevier
15. Dobson, J, Tweedie, A, Harvey et al: Finite element analysis simulations for ultrasonic array NDE inspections. *42nd Annual Review of Progress in Quantitative Nondestructive Evaluation: Incorporating the 6th European-American Workshop on Reliability of NDE.* 2016, vol. 1706, Melville, NY.